

International Conference on Space Optics—ICSO 2018

Chania, Greece

9–12 October 2018

Edited by Zoran Sodnik, Nikos Karafolas, and Bruno Cugny



Three years of optical satellite to ground links with the T-AOGS: data transmission and characterization of atmospheric conditions

K. Saucke

R. Mahn

P. Martin Pimentel

F. Heine

et al.



icso proceedings



3 Years of Optical Satellite to Ground Links with the T-AOGS: Data Transmission and Characterization of Atmospheric Conditions

K. Saucke^a, R. Mahn^a, P. Martin Pimentel^a, F. Heine^a,
R. Mata-Calvo^b, J. Sufo^{cb}, R. Barrios^b, A. Reeves^b, H. Bischl^b, H. Brandt^b, B. Matuz^b

^a*Tesat Spacecom, Backnang, Germany*

^b*Institute of Communications und Navigation, DLR, Wessling, Germany*

ABSTRACT

After more than 3 years of operational experiences with the Transportable Adaptive Optical Ground Station (T-AOGS) it is not any more the question whether optical communication through atmosphere is possible for Geo to ground applications. It is important to understand the performance of optical communication under different atmospheric conditions and which the key parameters are to improve simplicity, robustness and availability of optical bi-directional satellite to ground links (SGL). We report within this paper on the characterization of the atmospheric channel for ground to GEO optical communication without adaptive optics correction in the uplink. Besides the telemetry data of the space segment and the T-AOGS, also a special measurement campaign was carried out using the 1m telescope of the ESA-OGS in parallel. An outlook for further analysis and activities is given.

Keywords: optical space to ground communication, atmospheric channel characterization, feeder links, Alphasat, EDRS

1. INTRODUCTION

Since September 2015 the Transportable Adaptive Optical Ground Station (T-AOGS), co-located with the European Space Agency (ESA) Optical Ground Station on Tenerife, is operating and performing links with a LCT on the geostationary S/C Alphasat ([3],[4],[5]). Since than more than 900 satellite to ground links (SGLs) were carried out. These links were spread over 15 measurement campaigns covering all different seasons and different time of the day. The system is based on coherent homodyne optical communication with 1064 nm and binary phase shift keying (BPSK) modulation. With an clock rate of 2.8125 Gbps the standard user data rate is 1.8 Gbps, but can also be set to 600Mbps, matching the X-band down link performance. The performed links were used for different purposes:

- perform up-link and down-link communication
- perform special tests, e.g. pure ‘heterodyne links’: the TDPI-LCT remains in a heterodyne-status, no data communication is possible, but the receive optical intensity measurement is independent of the phase lock and thus not affected by fades that can unlock the RX communication chain. This type of links are used to measure the beam spread of the T-AOGS, to investigate the influence of the T-AOGS pointing on the scintillation seen at the space segment
- alignment and calibration links for the T-AOGS
- support for the test of other laser communication terminals [6]

The overall availability due to weather (high clouds, humidity, dust, heavy winds) is 60% -75%. It has to be considered that weather prediction was not part of the link planning.

The available measurement data can be classified in three categories:

- data measured on the TDPI-LCT and thus describing the up-link characteristic, data rate of 25 kHz
- data measured on the T-AOGS and thus describing the down-link characteristic, data rate of 5 kHz
- data measure at the ESA-OGS being equipped with a pupil images camera and a focal images camera

2. CHANNEL CHARACTERIZATION

Most of the data analyzed in the following are derived during a special measurement campaign from 13.05.2017 - 17.05.2017, were 21 links were performed at different time of the day. The weather conditions during these five days were better than average, nevertheless due to the different time of the day the optical channel varies.

2.1 Fried Parameter statistic

To estimate the turbulence conditions at a given site the Fried parameter r_0 can be measured as a statistical metric of the wavefront distortions. Here we use the focal speckle pattern method as described in [7] to estimate r_0 through the short-term tilt removed values of focal speckle sizes. The data were derived from recorded videos of the focal camera attached to the ESA-OGS 1 m telescope. The histogram of the observed Fried parameter is shown in figure 1. The data set is divided into two sub-sets: ‘homodyne’ and ‘heterodyne’. Homodyne collocates all data where up-communication was present (the TDP1 was in homodyne communication mode). Heterodyne collocates all data, where up-link communication was not present. This subset not only collects the data where up-link communication was not possible due to the quality of the optical channel, but also data, where up-link communication was not attempted. The Fried parameter measured on ground varies between 10 cm and 35 cm, while up-link communication is possible (figure 1, left). For figure 1, right, the heterodyne sub-set, it is assumed the main data peak around $r_0 = 14$ cm represent atmospheric conditions where up-link communication was not possible, while the data around $r_0 = 25$ cm up-link communication would have been possible.

This result leads to the following: the Fried parameter measured on ground is a rough reference but not a sufficient criteria for the up-link channel quality.

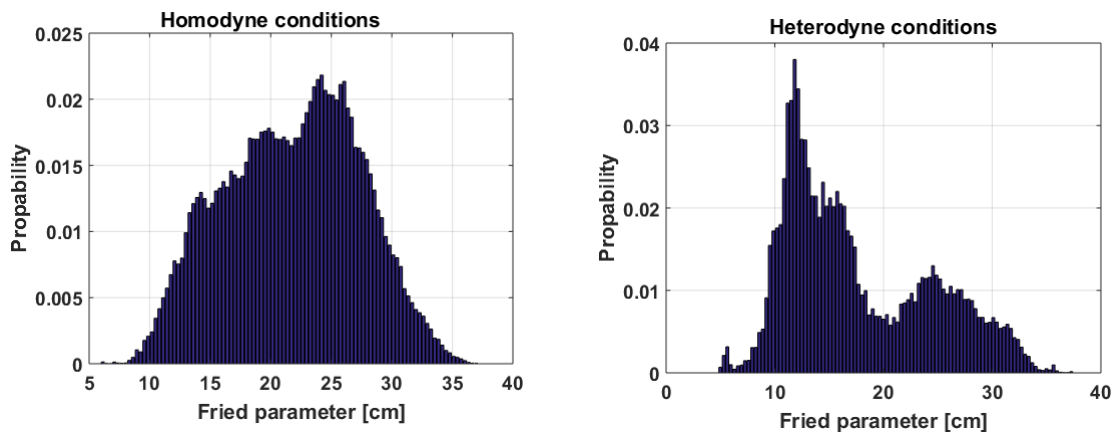


Figure 1. Histogram of Fried parameter seen during 21 link spread over the time 13.5.2018 - 17.05.2018. The y-axes is scaled such, that the area of each histogram is 1. The data-set is divided into two sub-sets: homodyne (left figure) where up-link communication was achieved, and heterodyne (right figure) where up-link communication was not achieved - either due to the quality of the atmospheric channel, or y intention / technical constraints.

The Fried parameter were also compared to theoretical results using different atmospherically model. The most straight forward way to compare the experimental data against theoretical values is by the median value, which is about 19 cm. It was seen that the Izaña models for day and night [7] underestimate the experimental data by a factor ~ 2 , while the Maui3 model [8] is closer to the experimental data giving a Fried of 24 cm. This observation has already been made during measurements performed in Tenerife by other research team [9].

2.2 Scintillation at the space segment and at the ground segment

The scintillation index σ_P for the light received at the space segment (Alphasat TDP1-LCT with 135 mm aperture) and at the ground segment (T-AOGS with 270 mm aperture) are derived from the measured optical power using the following formula:

$$\sigma_P^2 = \frac{\langle P_{RX}^2 \rangle - (P_{RX})^2}{(P_{RX})^2} \quad (1)$$

with P_{RX} being the optical receive power.

Figure 2 shows the scintillation seen at Alphasat TDPI-LCT and seen at the T-AOGS versus the Fried parameter measured on ground. Again the data is separated into two subsets ‘homodyne’ (figure 2, left), and ‘heterodyne’ (figure 2, right) as explained in the prior chapter.

The scintillation of the optical light at the space segment varies between 0.05 and 0.25 for the homodyne sub-set, where up-link communication was performed. For the heterodyne sub-set scintillation up to 0.4 were observed.

The scintillation index of the optical light measured at the ground segment is in most of the cases smaller by more than one decade. For the homodyne sub-set the scintillation measured within the 270mm aperture of the T-AOGS are between 0.002 and 0.07 with a mean value of ~ 0.005 . This is due to the asymmetry of the optical link: the space segment being far away from the atmospheric disturbances and larger spatial distances between the speckle patterns and the ground station being close to the atmospheric disturbances and short distances between the speckle patterns. Thus the ground station can reduce the effects of scintillation by aperture averaging [10].

There is no direct relation between the Fried parameter and the scintillation, also there slight decrease of the scintillation can be seen with higher Fried parameter.

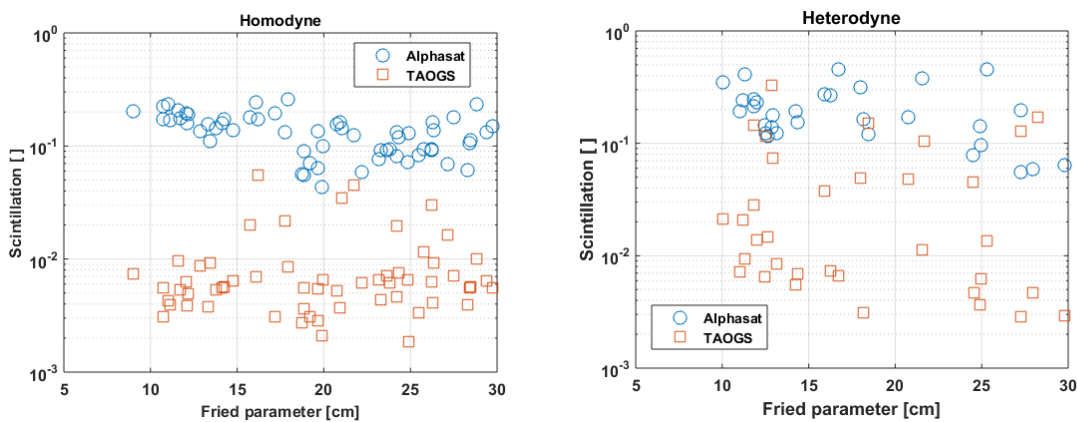


Figure 2. Scintillation seen at the space segment (TDPI-LCT on Alphasat) and at the ground segment (T-AOGS) in relation to the Fried-parameter measured on ground. Data separated into two subsets: homodyne (left figure) where up-link communication was achieved, and heterodyne (right figure) where up-link communication was not achieved - either due to the quality of the atmospheric channel, or y intention / technical constraints.

2.3 Pointing effecting the up-link, off-axis scintillation

In general: the intensity fluctuation seen at the receiver (in an up-link the light seen at the space segment, in a down-link the light seen at the ground segment) is not only dependent on the optical channel itself, but also on the characteristic of the sender (beam diameter and pointing (offset and jitter) and the receiver (tracking performance)). The TDPI-LCT shows a very constant pointing and tracking characteristic: small static TX/RX misalignment of $< 0.5\mu\text{rad}$, even within SGL a sub- μrad residual tracking error [4] and an overall pointing jitter of $< 2\mu\text{rad}$ has been measured previously. The T-AOGS on the other hand has, as operated at the moment, a TX/RX error of $10\mu\text{rad}$, up to $20\mu\text{rad}$. This is due to the fact that the TX/RX path are physically separated, thermal deformation of up to $100\mu\text{rad}$ can occur between the TX and RX path. The TX/RX alignment need to be adjusted by the T-AOGS operator for every link. This can only be done up to an accuracy of $\sim 10\mu\text{rad}$. However because of the uplink beam size of $2 \cdot w_0 \cdot 1.12 = 48\text{ mm}$ and the therefore larger divergence of $\sim 17\mu\text{rad}$ incl. truncation, the effect of static miss pointing from ground is less severe as in space, but not negligible. In the following we investigated the influence on such miss pointing of the T-AOGS on the scintillation seen at the space segment, which is of high interest for further understanding the turbulent satellite uplink channel. For intended and controlled miss-pointing the T-AOGS performed spiral TX pointing relative to the RX directing with increasing spiral radius. Figure 3 shows the time-line of the data. In figure 3, upper figure the received power with in the 135 mm aperture of the TDPI-LCT is shown. It decreases with larger angular separation between TX and RX. The red curve shows the angle according to the center point of the pointing CPA. If the pointing would be ideal, the plotted power in the upper figure would decrease monotonically. Hence it is assumed that the ideal pointing is off the center. An

estimated optimal pointing center is found by fitting the power vector to the CPA data. The distance between RX and TX is plot in the lower plot of figure 3 (blue). This distance is used for all further analysis

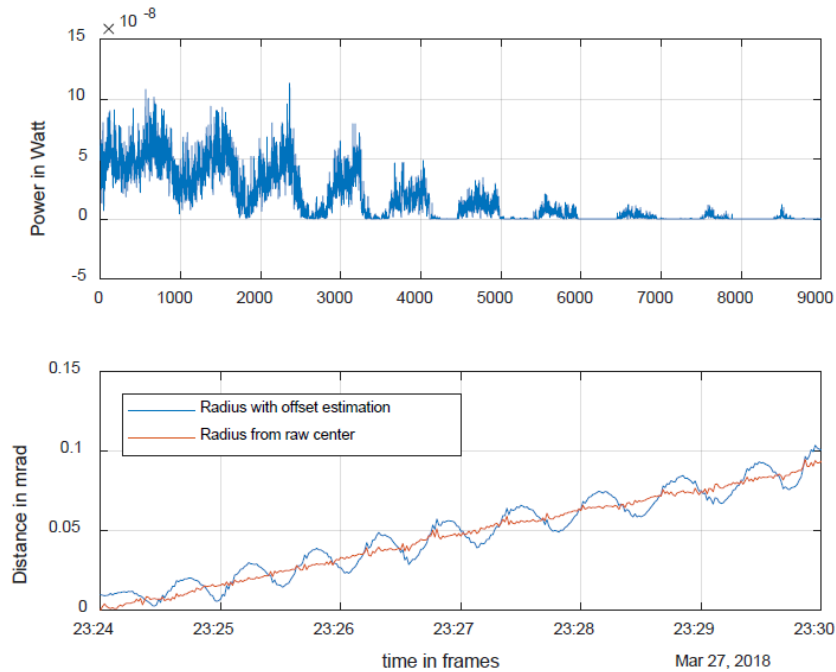


Figure 3. Measurement to determine off axis scintillation. The T-AOGS is performing a TX spiral scan relative to the RX tracking, including the PAA angle. The lower figure shows the rel. angular distance between TX and RX of the spiral scan. The red curve gives the distance to the uncorrected beam center of the CPA. The blue curve contains a beam center offset estimation, depending on the oscillations of the input power. The upper figure shows the optical power received at the space segment within the 135 mm aperture.

Within figure 4 the intensity and the scintillation seen at the space segment is plotted versus the off axis angle, the angle between the optimum TX direction (including the point ahead angle of 18 μ rad needed for a ground to space link) and the commanded TX direction.

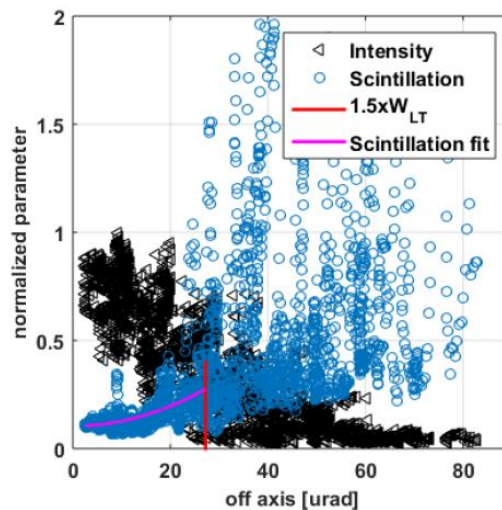


Figure 4. Intensity and scintillation seen at the TDP1-LCT versus intentional miss-pointing of the T-AOGS.

The received intensity is decreasing with larger of axis pointing. The T-AOGS was equipped with a TX beam diameter of $2 \cdot w_0 \cdot 1.12 = 48$ mm, which leads to, including truncation effects, a $1/e^2$ beam divergence radius of $17 \mu\text{rad}$. Due to the atmosphere it is slightly broadened to $\sim 18 \mu\text{rad}$ (w_{LT}). The scintillation is increasing with increasing off axis pointing. Up to roughly $28 \mu\text{rad}$, which is 1.5 times the far field beam divergence, the scintillation increase follows a parabolic fit. The increase of the scintillation is in the order of factor 2-3. For larger off axis angle the measurement and calculation method is not reliable any more due to low power and offset effects of the measured received power.

The data were also compared with theory and simulations given in [11] and it seems that the theory overestimates the radial component of scintillation.

2.4 Up-link channel fading analysis

The optical power received at the TDP1, e.g. shown in figure 5 and figure 7 contains surges (intensity increased relative to the mean intensity) and fades (intensity decreased relative to the mean intensity). Here we only investigate the fades. With respect to up-link communication the fades are the cause of bit errors or even link loss. Fades with the depth of -3dB, -6dB and -10dB relative to the mean power were investigated. The observed fade duration and number of fades per second are given.

First we show two example links, one with high mean power of 61.0 nW, the other with lower mean power of 43.7 nW seen within the 135 mm aperture of the TDP1-LCT. The T-AOGS TX power of ~ 50 W as well as the TX beam diameter of $2 \cdot w_0 \cdot 1.12 = 48$ mm were identical for all taken data.

2.4.1 Detailed example of a link with high received mean power of 61.0 nW

Figure 5 shows the timeline of the optical power received at TDP1. The recorded link time is 10min long. The link is almost homogenous with very little fade probability until $4 \cdot 10^6$ samples (first 2.5min) and a slight increase of fades with the time, e.g. due to T-AOGS miss pointing. The decrease in intensity at $\sim 12 \cdot 10^6$ samples is due to a short manual T-AOGS TX pointing alignment search.

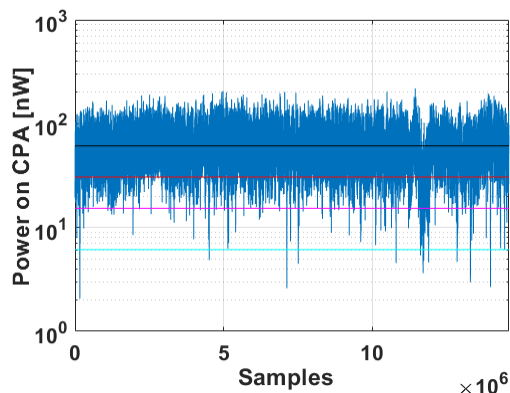


Figure 5. Power received within the 135 mm CPA aperture of the TDP1-LCT versus samples. The sample rate is 25 kHz. The recorded link time is 10 min long.

Statistical analysis onto the fades of this link is shown within Figure 6. The figure 6, left shows the number of fades/s as a histogram over the fades duration. The majority of the fades have a duration of 1 ms and shorter, and there are no fades longer than 100 ms. The figure 6, right shows the same data as CDF.

The fade statistic is summarized within table 1. Within this link there were 12 fades of -3dB per second and every ~ 12 s a fade of -10dB.

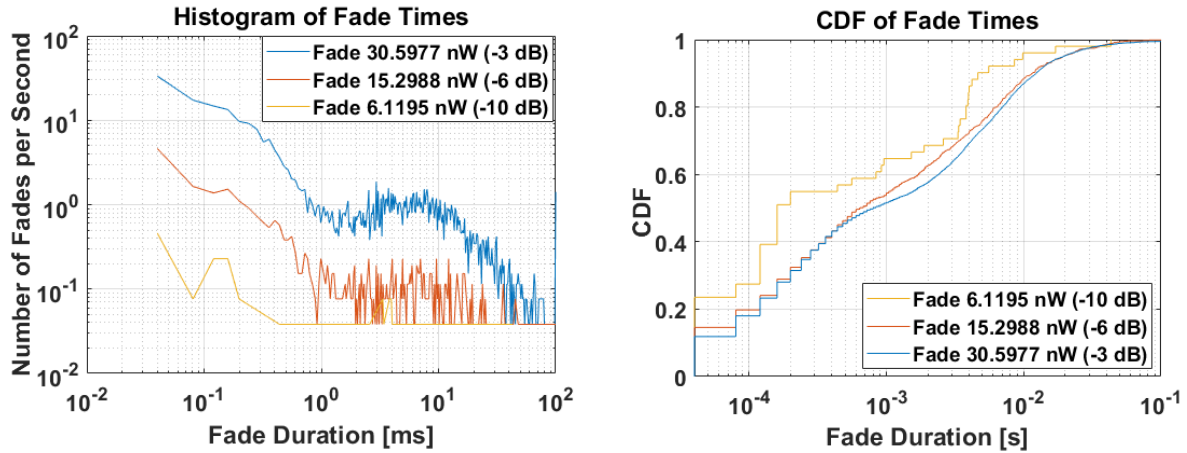


Figure 6. left: Occurring number of fades per second with a certain fade duration and depth; right: same data as CDF.

Table 1. fade statistic of the sample link

Fade Threshold	Mean Fade Time	Std. Dev. Fade Time	Number of Fades/s
30.60 nW (-3dB)	5.13 ms	14.35 ms	12.606
15.30 nW (-6dB)	4.29 ms	9.05 ms	1.421
6.12 nW (-10dB)	2.65 ms	6.57 ms	0.087

2.4.2 Overall statistics of up-link channel fading

In the following the up-link fading analysis, performed for all data collected in the measurement campaign from 13.05.2017 - 17.05.2017, is summarized and also set into relation with the Fried parameter measured by means of the focal camera attached to the ESA-OGS.

The mean fade duration of the up-link channel is almost not related to the R_0 measured within the down-link (see figure 5, right), whereas the number of fades per second have a slide tendency to decrease with larger R_0 (see figure 5, left). I.e. the length of the error correction code does not need to be adopted to in situ measured R_0 , but maybe the depth. Nevertheless the up-link channel could look quite different at other location of at other heights and dynamics (e.g. for optical links airplane to S/C).

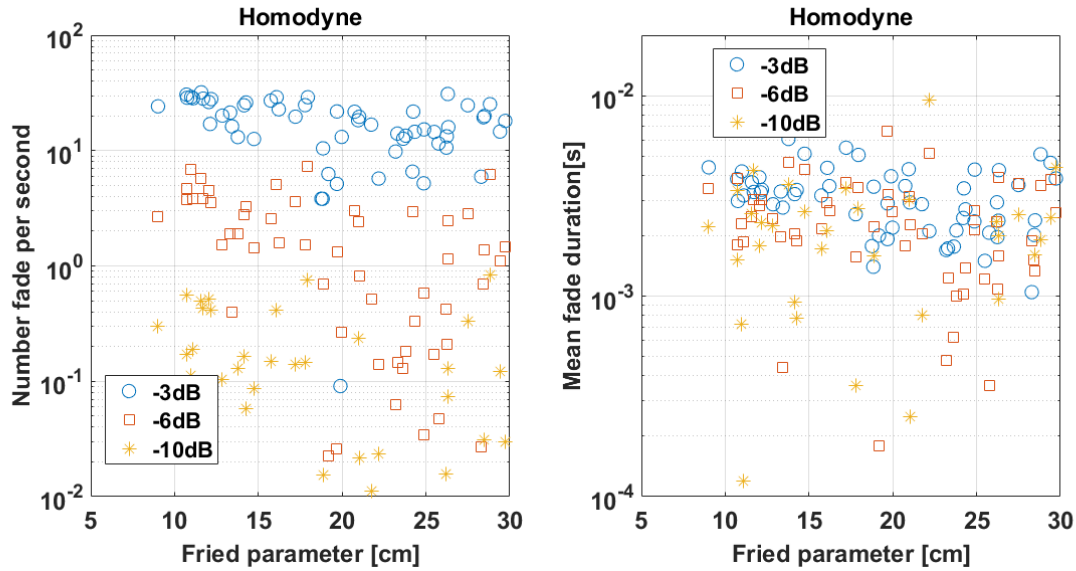


Figure 7. Fade statistics of the up-link channel (as seen on TDP1-LCT) during homodyne links (communication achieved) Number of fades per second (left) and mean fade duration (right) for -3dB, -6dB and -10db fades versus Fried parameter measured on ground (with ESA-OGS).

For homodyne links (figure 5 and figure 7, left), the mean fading time is between 2 to 3 ms for thresholds of -3 dB to -10 dB relative to its mean value. 80% of the times, the fading time remains below 4 ms and more than 95% of the times, the fading remains below 10 ms.

Comparing the fade statistic of the ‘homodyne’ sub-set (figure 5) and the ‘heterodyne’ sub-set (figure 6), it can be seen that for those times where up-link communication was not performed (‘heterodyne’), the number of fades per second are slightly higher, up to 60 per second, and the fade durations are slightly longer, up to 20ms. There are no fades longer than 100 ms.

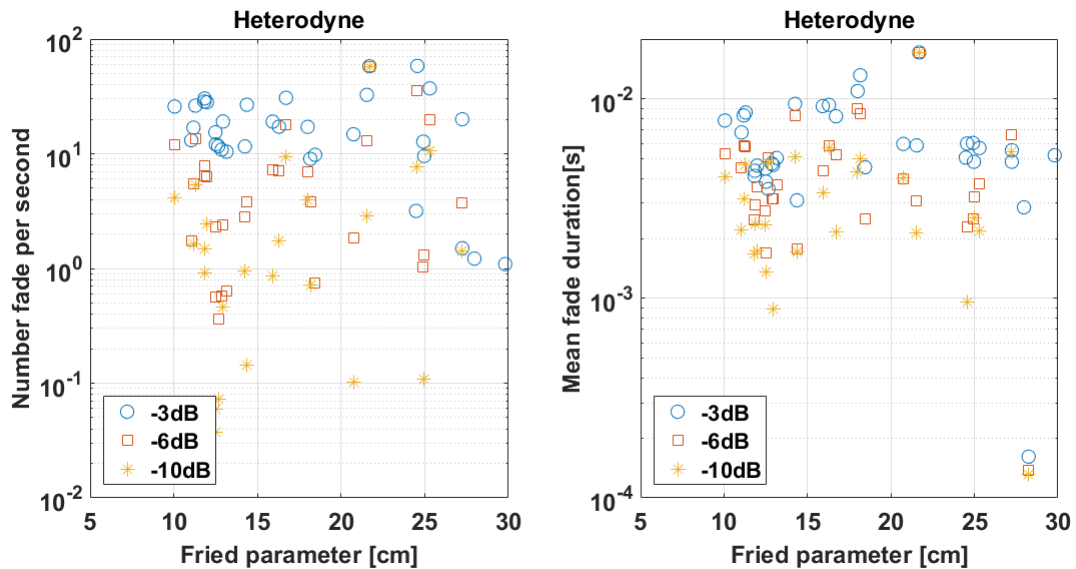


Figure 8. Fade statistics of the up-link channel (as seen on TDP1-LCT) during heterodyne links (no communication). Number of fades per second (left) and mean fade duration (right) for -3dB, -6dB and -10db fades versus Fried parameter measured on ground (with ESA-OGS).

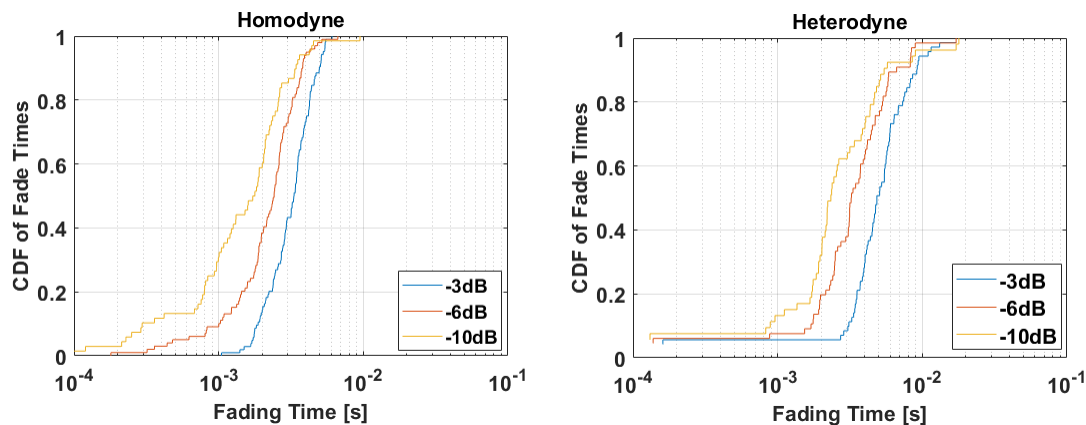


Figure 9. CDF of Fading time. left: for the homodyne sub-set, right: for the heterodyne sub-set.

The above fade statistics was done for fade depth of -3dB, -6dB, -10dB relative to the individual mean power of each link. This describes well a general quality of the atmosphere. From the point of view of the space segment the absolute power received and the fades given in absolute power is of high interest as well. Figure 8 shows the CDF of fade time for fades down to the absolute value of 40 nW, 20 nW and 10 nW within the 135 mm aperture of the TDP1-LCT. 40nW corresponds roughly to -44dBm, which is the design case of the TDP1-LCT for BER = 10⁻⁸. It can be seen (figure 8 left), that up-link communication (homodyne) was possible even through 10nW fades of up to 7 ms duration. The bit errors during these fades can be corrected by a forward error correction code specially adopted for the observed atmospheric characteristics as described within [12].

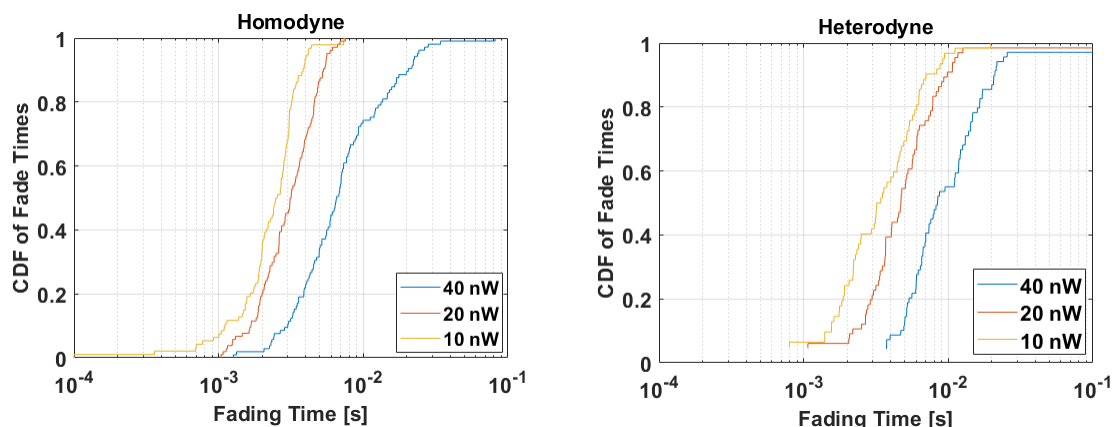


Figure 10. CDF of Fading time. left: for the homodyne sub-set, right: for the heterodyne sub-set. The fades are calculated for absolute power level: 40nW, 20nW and 10nW within the 135 mm aperture of the TDP1-LCT. 40nW is about -44dBm.

3. CONCLUSION AND OUTLOOK

Within this paper we reported on some characteristics optical light pathing the atmosphere, as measured for a GEO to ground link using the TDP1-LCT being at the geostationary S/C Alphasat and the T-AOGS being located at Izana, Tenerife. Some additional measurements were performed using the ESA-OGS. Data of one measurement campaign were analyzed regarding scintillation in the up- and down-link, fade statistic in the up-link and the influence of of-axis pointing of the T-AOGS onto the up-link channel. The data gathered within this campaign are also suited to obtain the Isoplanatic angle.

In order to achieve a more robust up-link communication, the T-AOGS will be retrofitted with a tracking system within the CPA100 transmit path. This should allow not only for a more automated operation but also for a better study of the

atmospheric conditions, as the TX/RX misalignment can be kept small and constant. It has to be noted that the primary target for the T-AOGS design was the down link performance using adaptive optics.

The TDPI-LCT has since May 2018 a new software with improved algorithm regarding SGLs. It is assumed that the homodyne phase lock will become even more robust, especially shorter times are needed for frequency re-acquisition.

More off-axis measurements of the scintillation behavior are necessary to formulate a theoretical model for satellite uplinks. This is of special interest for estimating the signal fluctuations due to miss-pointing or under residual beam-wander effects.

The up-link channel could look quite different at other location of at other heights and dynamics (e.g. for optical links airplane to S/C). In the near future it is foreseen to perform such measurements and analysis as well.

ACKNOWLEDGEMENTS

The activities described herein were carried out on behalf of the Space Administration of the German Aerospace Center (DLR e.V.) with funds from the German Federal Ministry of Economics and Energy with the reference number 50 YH 1640. We thank Synopta for hardware and software upgrades of the T-AOGS. Many thanks to Angel Alonso, IAC, who supports us on site. Many thanks also to Zoran Sodnik, ESA, to enable the parallel campaign using the ESA-OGS telescope.

REFERENCES

- [1] Fried, D.L., "Statistics of a Geometric Representation of Wavefront Distortion", *J. Opt. Soc. Am.* 55, 11, 1427–1431(1965).
- [2] Giggenbach, D., "Deriving an estimate for the Fried parameter in mobile optical transmission scenarios". *Appl. Opt.* 50, 222–226(2011).
- [3] Troendle, D. Saucke, K., Martín Pimentel, P., Motzigemba, M., Zech, H., Heine, F., "Optical Inter-Satellite and Feeder Links", *Proc. ICSOS (2017)*
- [4] Saucke, K. et al, "The TESAT Transportable Adaptive Optical Ground Station and the operational experiences", *Proceedings Volume 10562, International Conference on Space Optics — ICSO (2016)*
- [5] Saucke, K., Seiter, C., Heine, F., Gregory, M., Tröndle, D. Fischer, E. Berkefeld, T., Feriencik, M., Feriencik, M., Richter, I., Meyer, R., "The Tesat transportable adaptive optical ground station", *Proc. SPIE 9739, Free-Space Laser Communication and Atmospheric Propagation XXVIII, 973906 (15 March 2016)*
- [6] Martín Pimentel, P., Hoepcke, N., Saucke, K., Mahn, R., Marynowski, T., Heine, F. Meyer, R. and Lutzer, M., "Expanding Optical Communication Capabilities", *24th Ka and Broadband Communications Conference (Oct. 2018, to come)*
- [7] Comerón, A., Dios, F., Rodríguez, A., Rubio, J.A., Reyes, M. and Alonso, A., "Modeling of power fluctuations induced by refractive turbulence in a multiple-beam ground-to-satellite optical uplink." *Proc. SPIE, 58920O–58920O–10 (2005).*
- [8] Bradford, L.W. 2010. "Maui4: a 24 hour Haleakala turbulence profile", *Proceedings of the AMOS Technical Conference (2010).*
- [9] Yura, H.T. and Kozlowski, D.A., "Low Earth orbit satellite-to-ground optical scintillation - comparison of experimental observations and theoretical predictions", *Opt. Lett.* 36, 13 (Jul. 2011), 2507–2509.
- [10] Perlot, N., Fritzsche, D., "Aperture averaging: theory and measurements" *Proceedings Volume 5338, Free-Space Laser Communication Technologies XVI; (2004).*
- [11] Andrews, L.C. and Phillips, R.L. "Recent results on optical scintillation in the presence of beam wander." *Proc. SPIE, 687802–14(2008).*
- [12] Heine, F., Martín Pimentel, P., Rochow, C., Saucke, K., Tröndle, D., Lutzer, M., Meyer, R., Bischl, H., Matuz, B., "The European data relay system and Alphasat to T-AOGS space to ground links, status and achievements in 2017", *Proc. SPIE 10524, Free-Space Laser Communication and Atmospheric Propagation XXX, 105240T (15 February 2018).*